
X-Ray Variability of AGN and Relationship to Galactic Black Hole Binary Systems

Ian M^cHardy¹

School of Physics and Astronomy, University of Southampton, Southampton S017 1BJ, UK imh@astro.soton.ac.uk

Summary. Over the last 12 years, AGN monitoring by *RXTE* has revolutionised our understanding of the X-ray variability of AGN, of the relationship between AGN and Galactic black hole X-ray binaries (BHBs) and hence of the accretion process itself, which fuels the emission in AGN and BHBs and is the major source of power in the universe. In this paper I review our current understanding of these topics.

I begin by considering whether AGN and BHBs show the same X-ray spectral-timing ‘states’ (e.g. low-flux, hard-spectrum or ‘hard’ and high-flux, soft-spectrum or ‘soft’). Observational selection effects mean that most of the AGN which we have monitored will probably be ‘soft state’ objects, but AGN are found in the other BHB states, although possibly with different critical transition accretion rates.

I examine timescale scaling relationships between AGN and BHBs. I show that characteristic power spectral ‘bend’ timescales, T_B , scale approximately with black hole mass, M_{BH} , but inversely with accretion rate, \dot{m}_E (in units of the Eddington accretion rate) probably signifying that T_B arises at the inner edge of the accretion disc. The relationship $T_B \propto M_{BH}/\dot{m}_E$ is a good fit, implying that no other potential variable, e.g. black hole spin, varies significantly. Lags between hard and soft X-ray bands as a function of Fourier timescale follow similar patterns in AGN and BHBs.

I show how our improved understanding of X-ray variability enables us to understand larger scale properties of AGN. For example, the width of the H_β optical emission line, V , scales as $T_B^{1/4}$, providing a natural explanation of the observed small black hole masses in Narrow Line Seyfert Galaxies; if M_{BH} were large then, as $T_B \propto M_{BH}/\dot{m}_E$, we would require $\dot{m}_E > 1$ to obtain narrow lines.

I note that the rms X-ray variability scales linearly with flux in both AGN and BHBs, indicating that the amplitude of the shorter timescale variations is modulated by that of the longer timescale variations, ruling out simple shot-noise variability models. Blazars follow approximately the same pattern. The variations may therefore arise in the accretion disc and propagate inwards until they hit, and modulate, the X-ray emission region which, in the case of blazars, lies in a relativistic jet.

Short timescale (weeks) optical variability arises from reprocessing of X-rays in the accretion disc, providing a diagnostic of X-ray source geometry. On longer timescales, variations in the disc accretion rate may dominate optical variations.

AGN X-ray monitoring has greatly increased our understanding of the accretion process and there is a strong case for continued monitoring with future observatories.

1 Introduction

Understanding the relationship between AGN, which are powered by accretion onto supermassive black holes, and the much smaller Galactic black hole binary systems (BHBs) is currently one of the major research areas in high energy astrophysics. Possible similarities between AGN and BHBs have been mooted ever since the late 70's and early 80's when it was first realised that they were both black hole systems [e.g 86]. However comparison of their X-ray variability properties provided the first quantitative method for this comparison [49]. More recently considerable attention has been devoted to the jet properties of black hole systems and a strong scaling has been shown by means of comparing radio and X-ray luminosities [44, 23]. However here I concentrate on the considerable insight which can be gained regarding the scaling between AGN and BHBs by studying their X-ray timing similarities.

I begin this review with a discussion of AGN 'states', as we must be sure, when comparing AGN with BHBs, that we are comparing like with like. I then discuss characteristic X-ray variability timescales and how they scale with mass and accretion rate. I then show how larger scale AGN properties, e.g. AGN optical permitted line width, are related to the small scale accretion properties. I discuss models for the origin of the variability and show how the variability of blazars fits the same pattern as for Seyfert galaxies, showing that the source of the X-rays is separated from the source of the variations, which may be the same in all accreting objects. The long AGN X-ray monitoring programmes which were set up to enable us to compare AGN and BHB X-ray variability properties have also allowed us, through correlated monitoring programmes in other wavebands, to understand a little about what drives the optical variability of AGN. I therefore conclude this review with an examination of that topic.

2 AGN X-ray Variability and AGN 'states'

2.1 States of Galactic Black Hole X-ray Binary Systems

BHBs are found in a number of 'states', originally defined in terms of their medium energy (2-10 keV) X-ray flux and spectral hardness. These states are discussed fully elsewhere in this volume [8, 24] but, for completeness here, and at the risk of some over-simplification, I briefly summarise the properties of the most commonly found states, i.e. the 'hard', 'soft' and 'VHS' states.

In the 'hard' state the medium energy X-ray flux is low and the spectrum is hard. In the 'soft' state, the medium energy X-ray flux is high and the spectrum soft. The main spectral characteristic of the very high state (VHS), sometimes also known as the high intermediate state, is that the X-ray flux is very high. The spectrum is intermediate in hardness between the hard and soft states. The accretion rate rises as we go from the hard to soft to VHS states. The X-ray timing properties of the different spectral states are also very different, and quite characteristic and may, in fact, provide a better state discriminant than the spectral properties.

X-ray variability is usually quantified in terms of the power spectral density (PSD) of the X-ray light curve. In Cyg X-1 there is a large amplitude of variability in the soft-intermediate and soft states and the PSD is well described by a simple

bending powerlaw. At high frequencies the power spectral slope is -2 or steeper (i.e. $P(\nu) \propto \nu^{-\alpha}$ with $\alpha \geq 2$) bending, below a characteristic frequency ν_B (or timescale T_B) to a slope $\alpha \simeq 1$ [16, 55]. In most other BHBs, eg GX 339-4 [7], which typically differ from Cyg X-1 in reaching the soft state only during very high accretion rate transient outbursts but then reaching a more pronounced soft state, the variable component is swamped by a quiescent thermal component and so is very hard to quantify. However the PSD of the weak variable component, when measurable, is consistent with the shape seen for Cyg X-1.

In the hard state the PSD can also be approximated by bending powerlaws, and the high frequency bend is also seen. In addition, a second bend to a slope of $\alpha = 0$ is seen approximately 1.5 to 2 decades below the high frequency bend. However in the hard state, BHB PSDs are better described by a combination of Lorentzian shaped components [59], with prominent components being located at approximately the bends in the bending powerlaw approximation to the PSD. In the very high state and, indeed, in any state apart from the soft state, the PSD can be described by the sum of Lorentzian components, as in the hard state. However in the very high state, the corresponding Lorentzian frequencies are higher than in the hard state.

2.2 Quantifying AGN States by Power Spectral Analysis

AGN typically have X-ray spectra similar to those of hard state BHBs (i.e. photon indices ~ 2), and much harder than soft state BHBs. [Note that, unless specifically mentioned to the contrary, by ‘AGN’ I mean an active galaxy, such as a Seyfert galaxy, where the emission does not come from a relativistic jet. Relativistically beamed AGN, i.e. blazars, are discussed in Sect. 7.] Simple spectra do not provide a particularly direct means of state comparison as, in soft state BHBs, the very hot accretion disc leads to a large, soft spectrum, thermal component which dominates the medium energy emission. In AGN the accretion disc is much cooler and so does not affect the medium energy flux, even at high accretion rates. However if one can disentangle the relative contribution of the accretion disc from the total luminosity then AGN and BHB do seem to occupy broadly similar regions of disc-fraction/luminosity diagrams [e.g. 33, 24]. Nonetheless timing properties may provide a cleaner and simpler state discriminant and means of comparing AGN with BHBs. However there are considerable difficulties in measuring AGN PSDs over a wide enough frequency range that the equivalent of the bends seen in BHB PSDs may be found. Assuming to first order that system sizes, and hence most relevant timescales, will scale with black hole mass, M_{BH} , then as $\nu_B \sim 10\text{Hz}$ for the BHB Cyg X-1 in the high state [$M_{BH} \sim 10 - 20M_{\odot}$; 31, 88], we might expect $\nu_B \sim 10^{-7}\text{Hz}$ for an AGN with $M_{BH} = 10^8 M_{\odot}$. To measure such a bend requires a light curve stretching over a number of years.

The first really detailed observations of AGN X-ray variability were made by EXOSAT. In the case of NGC 4051 [36] and NGC 5506 [47], variability on timescales of less than $\sim\text{day}$ was shown to be scale-invariant, initially dashing hopes of finding some characteristic timescale from which black hole masses could be deduced. However by combining the EXOSAT observation of NGC 5506 with archival observations from a variety of satellites, it was possible to make a PSD covering timescales from $\sim\text{years}$ to $\sim\text{minutes}$. Although poorly determined on long timescales, the PSD did roughly resemble the PSD of a BHB and was sufficient to show that the scale invariance which prevailed on timescales shorter than a day broke down at timescales of

around a few days to a week [49, 50]. The bend timescale was broadly consistent with linear scaling with mass. But the long timescale data were very poor. Subsequent archival searches produced a measurement of a bend frequency in NGC 4151 [64] but again the long timescale data were poorly sampled. However the long timescale monitoring of AGN, on which the production of high quality PSDs relies, was revolutionised in late 1995 with the launch of the *RXTE* which was specifically designed for rapid slewing, allowing for monitoring on a variety of timescales from hours to years. As a result a number of groups began monitoring AGN. Long timescale PSDs of good quality were made and reliable bend frequencies were measured for a number of AGN [eg 54, 20].

Power Spectral analysis of irregularly sampled data

Determining the shape of AGN PSDs from sampling that is usually discrete, and irregular is not trivial. Fourier analysis of the raw observational data will result in the true underlying PSD being distorted by the window function of the sampling pattern. The non-continuous nature of most monitoring observations means that high frequency power is not properly sampled, which results in that power being ‘aliased’, or reflected, back to lower frequencies. Also, as the overall light curves have a finite length, low frequency power is not properly measured and so additional spurious power leaks into the PSD from low frequencies. This latter effect is known as red noise leak. The shape of the true underlying PSD can, however, be estimated by modelling. The procedure which we use is called PSRESP [83]. This procedure builds on earlier work (the ‘response’ method, [18]) and other previous authors have also used a similar method to analyse AGN X-ray variability [27]. In PSRESP we assume a model form for the underlying PSD and, using a now standard prescription [75], a light curve is then simulated. This light curve is folded through the real observational sampling pattern and a ‘dirty’ simulated PSD is produced. This procedure is repeated many times to establish an average model dirty PSD and to establish its errors. Observations from a number of different observatories (e.g. *RXTE* *XMM-Newton* *ASCA*) can be modeled simultaneously. The real, observed, dirty PSD is then compared with the dirty model average and the model parameters are adjusted until the best fit is obtained.

Using PSRESP we have determined the overall PSD shapes of a number of AGN, covering timescales from years to tens of seconds. [e.g. 83, 55, 52, 82]. In only one case (Akn 564, described below) do we find evidence for more than one bend in the PSD. In all other cases we find only one bend, from $\alpha = 2$ at high frequencies to $\alpha = 1$ at lower frequencies. In NGC 4051 [55] and MCG-6-30-15 [52] the slope of $\alpha = 1$ continues for at least 4 decades below the upper bend and in a number of other AGN (e.g. NGC 3227, [82]) the slope can be traced for at least 3 decades. In such cases we can be reasonably sure that a hard state PSD is ruled out and a soft state PSD is required. In other cases there may not be sufficient low frequency data to distinguish between hard and soft states but in all cases a soft state PSD is consistent with the data.

The lack of hard state AGN PSDs may, however, just be a selection effect. Most of the AGN that have recently been monitored are X-ray bright and have moderate accretion rates (typically above a few per cent of the Eddington accretion rate, \dot{m}_E). In BHs, whenever the accretion rate is below $\sim 0.02 \dot{m}_E$, the sources are found in the hard state. Although hard states are also found above $\sim 0.02 \dot{m}_E$, no soft states

are found below that accretion rate. Thus the finding that almost all AGN PSDs may be soft state PSDs is consistent with the expectation based on their accretion rates. It is also possible that the transition accretion rate between the hard and soft states is different in AGN. Soft states are associated with an optically thick accretion disc reaching close in to the black hole. In the lower temperature discs around more massive black holes (i.e. AGN) it is possible that the optically thick part of the accretion disc might survive without evaporation, at the same accretion rate, at smaller radii than in the hotter discs around BHBs. Thus the transition accretion rate might be lower around AGN. However the data do not yet allow us to test this possibility.

There had been a tentative suggestion that there might be a second bend, at low frequencies, in the PSD of NGC 3783 and hence that it might be a hard state system [42]. As NGC 3783 does not have a particularly low accretion rate ($\sim 0.07 \dot{m}_E$), this suggestion was a little puzzling. However our further observations [73] show that, in fact, NGC 3783 is another soft state AGN.

2.3 The Unusual case of Akn 564 - A very high state AGN

The finding of a VHS PSD in a high accretion rate AGN would significantly strengthen the growing link between AGN and BHBs. Arakelian 564 is one of the highest accretion rate AGN known ($\dot{m}_E \sim 1$) and is the only AGN for which there is presently good evidence that its PSD contains more than one bend. From observations with *RXTE*, evidence for a low frequency bend was presented [68] and evidence for a second bend, at high frequencies, was also found from analysis of *ASCA* observations [62]. The combined *RXTE* and *ASCA* PSD was interpreted as a hard state PSD [62] although it was noted that the frequency of the high frequency bend did not scale linearly with mass to that of the hard state of the archetypal BHB Cyg X-1; the frequency difference is too small. However proper modeling of the combined long and short timescale PSD was hampered by the gaps which occur in the *ASCA* light curves, and hence in the PSD, at the orbital period (~ 5460 s). We therefore made a 100ksec continuous observation with *XMM-Newton* to fill that gap in the PSD and the resulting overall *XMM-Newton* *ASCA* and *RXTE* PSD is shown in Fig. 1, bottom panel. Although the PSD of Akn 564 can be fitted with a doubly-bending powerlaw as well as with two Lorentzian components, strong support for the Lorentzian interpretation is given by the spectrum of the lags between the hard and soft X-ray bands. It has long been noted in both BHBs [e.g. 60] and AGN [e.g. 65, 55] that the X-ray emission in the harder energy bands usually lags behind that in the softer bands and that the lag increases with increasing energy separation between the bands. However if we split the light curves into components of different Fourier frequency we can measure the lag as a function of Fourier frequency, i.e. we can determine the lag spectrum. Although I do not discuss it here, the degree of correlation between light curves is known as the coherence which, together with the lags, can provide a very useful diagnostic of the source geometry and emission mechanism. The calculation of lags and coherence is known as cross-spectral analysis and a full description of the technique and its applications is given elsewhere [85].

In BHBs where the PSD is well described by the sum of Lorentzian components, i.e. in every state apart from the soft state, it is found that the lags are reasonably constant over the frequency range where the PSD is dominated by any one

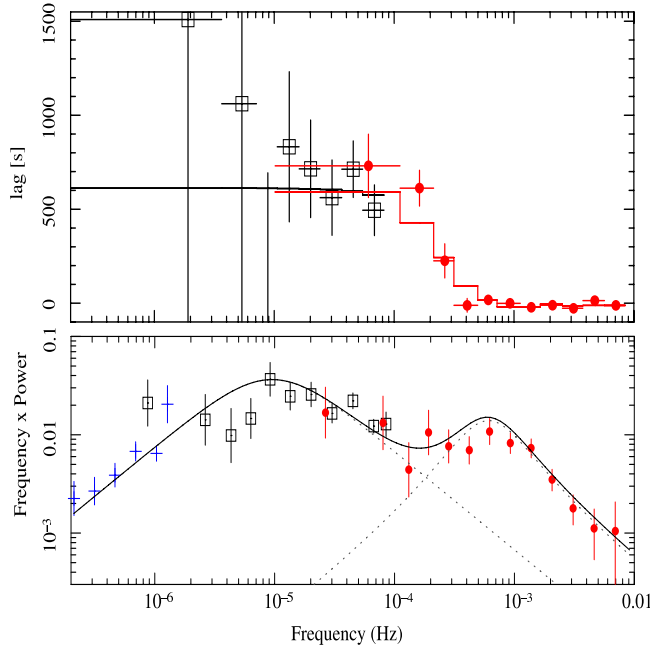


Fig. 1. Top panel: Lag between the hard (2-10 keV) and soft (0.5-2 keV) X-ray bands as a function of Fourier frequency, for Akn 564. A positive lag means that the hard band lags the soft. Above 10^{-3} Hz the lags become slightly negative (-11 ± 4.3 s), i.e. the soft band lags the hard band. Bottom panel: PSD of Akn 564 showing a fit to the two-Lorentzian model [51]. Note how the cross-over frequency between the two Lorentzians corresponds to the frequency at which the lags rapidly change.

Lorentzian component, but the lags change abruptly at the frequencies at which the PSD changes from one Lorentzian component to the next. In most AGN the PSD and lag spectra are not defined well enough to distinguish different Lorentzian components but for Akn 564 we can measure the lag spectrum (Fig. 1, top panel). We see that the lag changes rapidly from one fairly constant level to another at the frequency where the PSD changes from one Lorentzian to another. Given the extremely high accretion rate of Akn 564, we interpret these observations as strongly supporting the VHS, rather than hard state, interpretation. We also note that, at the highest frequencies (above 10^{-3} Hz), the lags become slightly negative, i.e. the soft band lags the hard band. One possible explanation is that, at these frequencies, which may come from the very innermost part of the accretion disc, the soft X-rays arise mainly from reprocessing of harder X-rays by the accretion disc (see Sect. 6.3).

Ton S180 In our recent PSD survey of 32 well observed AGN (Summons et al in preparation) the only AGN besides Akn 564 for which there are reasonable hints that a double-Lorentzian, rather than a single bending powerlaw model, is required is Ton S180 (Fig 2). Interestingly Ton S180 has, like Akn 564, an accretion rate close to the Eddington limit and so may very well be another VHS system. As with

Ark 564, we have calculated the lag spectrum but the data are not as good as for Ark 564. The lags are, however, consistent with a VHS interpretation, as in Ark 564.

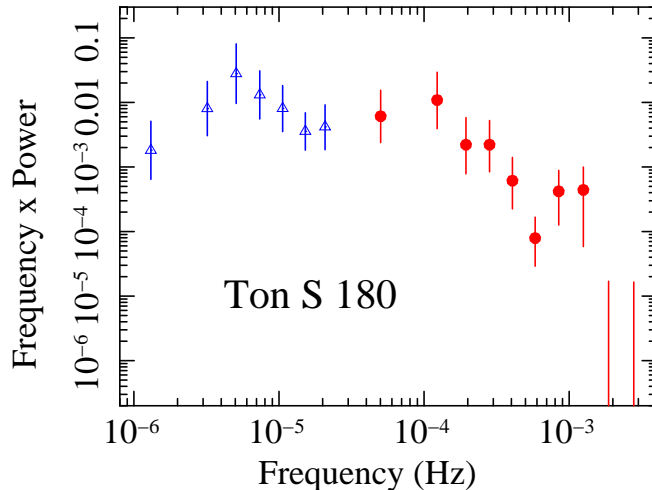


Fig. 2. Combined *RXTE* and *ASCA* PSD of Ton S180, unfolded from the distortions introduced by the sampling pattern, assuming a simple model of a powerlaw with a bend at high frequencies. Two large bumps are seen in the residuals which can be fitted equally well with two Lorentzian-shaped components (Summons et al., in preparation)

2.4 Periodicities in AGN

Although broad Lorentzian features can be fitted to the PSDs of Akn 564 and Ton S180 there have been, until very recently, no believable detections of highly coherent periodicities in AGN. However one periodicity of high quality factor ($Q > 16$) has now been found in the NLS1 RE J1034+396 (Fig 3, from [25]). The periodicity does change in character during the observation with slight shifts in times of minimum and variations in amplitude so it is very similar to the quasi-periodic oscillations (QPOs) seen in BHBs [e.g. 70].

The reason that a narrow QPO is found in RE J1034+396 is not known. It has a high accretion rate, but so too does Akn 564 and Ton S180. It has been suggested that perhaps the phenomenon is transient as in BHBs [25] and the observers were just very lucky. Alternatively it may have something to do with the overall spectral shape of RE J1034+396 which is unique, even for an NLS1, peaking in the far UV. Whatever the reason, this observation is very important as it shows that the X-ray variability similarities between AGN and BHB extend to almost all known phenomena. It also enables us to estimate the black hole mass. In BHBs there is a tentative relationship between the frequency of the high frequency QPOs and the mass, $f_0 = 931(M/M_\odot)\text{Hz}$ [e.g. 70] where f_0 is the fundamental frequency of the pair of high frequency QPOs whose frequency ratio is $2f : 3f$. In RE J1034+396

then (and depending a little on which of the 2 high frequency QPOs we think the observed periodicity is) we can estimate a mass around $10^7 M_{\odot}$.

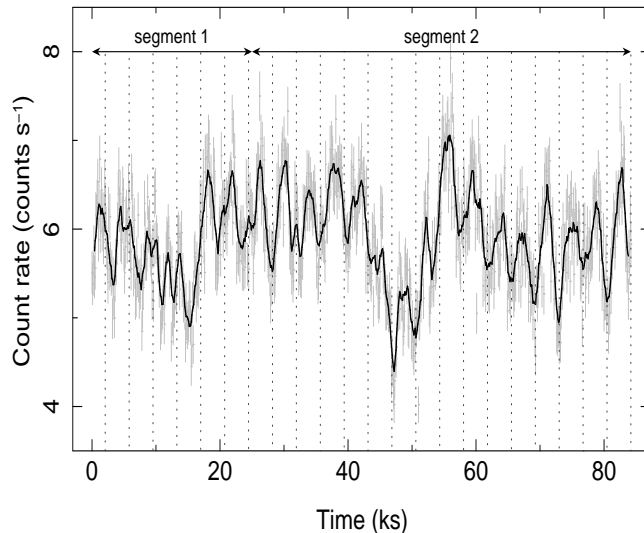


Fig. 3. *XMM-Newton* 0.3-10 keV light curve of RE J1034+396 [25]. The thick black line represents the running average over 9 bins. The vertical dotted lines show the expected times of minima obtained from folding segment 2 with the period 3733s.

3 Scaling characteristic timescales with mass and accretion rate

The early suggestions of a scaling of T_B with M_{BH} [50, 64] were supported by the first results from the *RXTE* monitoring programmes [e.g. 54, 20, 83, 42]. However once T_B had been measured in more than just a handful of AGN it was clear that there was much more spread in the T_B vs. M_{BH} relationship than could be accounted for just by observational error. Interestingly it was noted that for a given M_{BH} , the narrow line Seyfert 1 galaxies (NLS1s) had shorter values of T_B than broad line AGN and so it was suggested that accretion rate, as well as M_{BH} , might also affect the value of T_B [55, 52, 82]. The reason for the dependence on accretion rate was not clear but one possibility was that, if T_B is somehow associated with the inner edge of the optically thick part of the accretion disc, then if that edge moves closer to the black hole when the accretion rate rises [21], then T_B would decrease. Also, the increase in accretion rate would lead to an increase in luminosity and hence in an increase in the inner radius of the broad line region (R_{BLR}), and therefore in a decrease of the typical velocities, or widths, associated with the emission lines [52].

3.1 Fitting the timing scaling relationship for soft-state objects

In order to properly quantify the dependence of T_B on M_{BH} and \dot{m}_E , and motivated by the approximate linear relationship between T_B and \dot{m}_E and the approximate inverse relationship between T_B and \dot{m}_E we hypothesised that

$$\log T_B = A \log M_{BH} - B \log L_{bol} + C$$

where L_{bol} is the bolometric luminosity, and performed a simple 3D parameter grid-search to determine the values of the parameters A, B and C . As the AGN under consideration were, in all cases where the PSD was well defined, soft-state objects, then $\dot{m}_E \sim L_{bol}/L_{Edd}$. However we preferred to fit to L_{bol} rather than \dot{m}_E as L_{bol} is an observable, rather than a derived, quantity. The best fit to a sample of 10 AGN was $A = 2.17^{+0.32}_{-0.25}$, $B = 0.90^{+0.3}_{-0.2}$ and $C = -2.42^{+0.22}_{-0.25}$ [53].

In order to determine whether the same scaling extends down to BHBs we included two bright BHBs Cyg X-1 (and GRS 1915+105) in radio-quiet states where, for proper comparison with the AGN, their high frequency PSDs are well described by the same cut-off, or bending power-law model which best describes AGN and where broad band X-ray flux provides a good measurement of bolometric luminosity. For Cyg X-1, we combined measurements of T_B [5] with simultaneous measurement of the bolometric luminosity [87] over a range of luminosities. For GRS 1915+105, we measured an average T_B from the original X-ray data, and determined L_{bol} from the published fluxes [77] and generally accepted distance (11 kpc). For the combined fit to the 10 AGN and the two BHBs, we find complete consistency with the fit to the AGN on their own, i.e. $A = 2.1 \pm 0.15$, $B = 0.98 \pm 0.15$ and $C = -2.32 \pm 0.2$. The confidence contours for the fit to the AGN on their own and to the combined AGN and BHB sample are shown in Fig 4. We can see that, even at the 1σ (i.e. 68% confidence) level, the contours for the AGN on their own, and for the combined AGN and BHB sample, completely overlap (as do the offset constants, C). Thus we answer a long-standing question and show, using a self-consistently derived set of AGN and BHB timing data, that over a range of $\sim 10^8$ in mass and $\sim 10^3$ in accretion rate, AGN behave just like scaled-up BHBs. Assuming $\dot{m}_E = L_{bol}/L_{Edd}$, then $T_B \propto M_{BH}^{1.12}/\dot{m}_E^{0.98}$.

We can see how well the scaling relationship fits the data by comparing the observed bend timescales with the values predicted by the best fit parameters (Fig 5). The only noticeable outlier is NGC 5506 (at $\log T_{predicted} = +1.3$). However we note that the black hole mass estimate for NGC 5506 ($10^8 M_\odot$) which we used [53] is based on the width of the [OIII] lines, which is only a secondary mass estimator. The resultant implied accretion rate (2.5% \dot{m}_E) is surprisingly low given its recent classification, from the width of the IR P_β line, as an obscured NLS1 [56]. However using the recently measured width of its stellar absorption lines [28], a smaller mass (few $\times 10^6 M_\odot$) is derived. With that lower mass, NGC 5506 lies much closer to the best-fit line.

3.2 Constraint on black hole spin

In the fits discussed above, the best-fit reduced χ^2 was very close to unity. These fits were performed without introducing any additional systematic error into the fit, but purely by using the best estimates of the observational errors. In many such fits

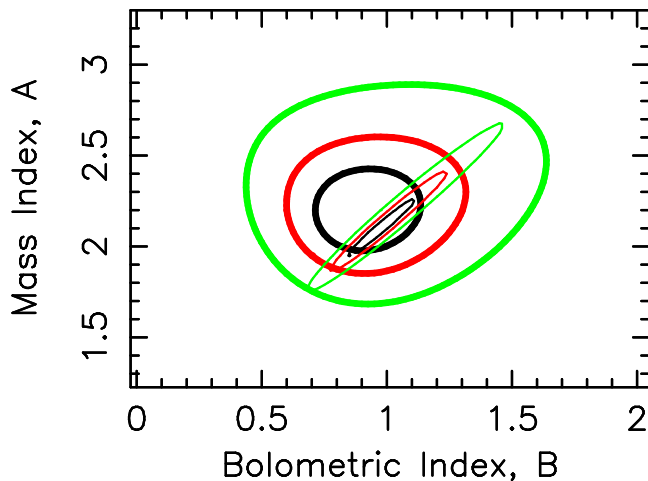


Fig. 4. Assuming a relationship between the PSD bend timescale, T_B the black hole mass, M_{BH} and the bolometric luminosity, L_{bol} of the form $\text{Log } T_B = A \text{Log } M_{BH} - B \text{Log } L_{bol} + C$, where C is a constant, we present here the 68% (black), 90% (red) and 95% (green) confidence contours for A and B . The thick contours are derived from a fit to 10 AGN only. The thin contours also include the BHBs Cyg X-1 and GRS 1915+105 in their soft (radio quiet) states. Note how the contours overlap completely, even at the 68% confidence level.

an unknown additional error has to be introduced to bring the reduced χ^2 down to unity, but we do not require any additional source of uncertainty. The implication is that no other parameter, which we do not include in the fit, varies greatly from object to object. One parameter which could conceivably affect T_B is black hole spin. In faster spinning black holes, the innermost stable orbit is closer to the black hole. Thus if T_B is related to the radius of the inner edge of the accretion disc, and if that edge reaches right up to the last stable orbit, then T_B might be lower in faster spinning black holes. The implication of the good quality of the present fit is that spin does not vary greatly from object to object. Thus if some X-ray emitting black holes are considered, from the width of their Fe K_α emission lines, to be maximally spinning [22], then probably they all are.

3.3 Scaling relationship for hard-state objects

An inverse dependence of a characteristic timescale on accretion rate had been noted elsewhere [45]. There it was noted that the frequency of the highest frequency lorentzian component, ν_{high} , in the hard-state PSD of the BHB GX 339-4, varied with radio luminosity, L_R , approximately as $\nu_{high} \propto L_R^{1.4}$. In standard jet models [e.g. 10] the total power in the jet, $L_J, \propto L_R^{1.4}$. Assuming that $L_J \propto \dot{m}_E$, then it is expected that $\nu_{high} \propto \dot{m}_E$ [45].

A similar scaling of characteristic timescale with accretion rate is seen in hard state observations of the BHB XTE J1550-564. In their Fig.3, Done et al [17] plot ν_{high} against a parameter which they label “ L_{bol} ”. However this parameter is derived

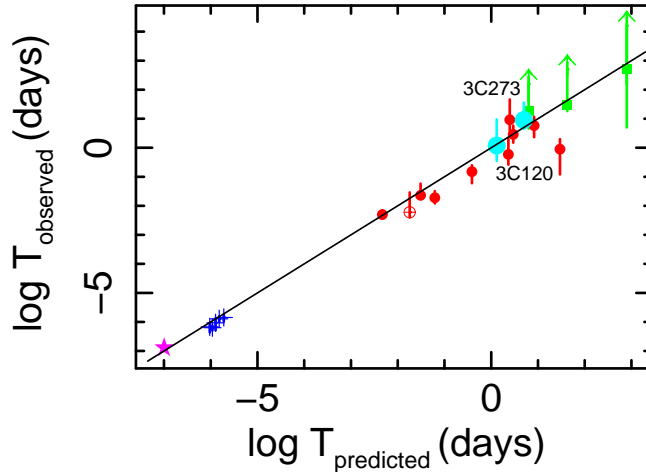


Fig. 5. Log of the observed vs. the predicted PSD bend timescales (in units of days), using the best-fit relationship derived from Fig. 4. The star on the lower left is GRS 1915+105, the crosses are Cyg X-1 and the circles are the AGN which were included in the fit. The three squares, whose upper bend timescales are unbounded, are AGN which were not included in the fit. However it can be seen that the measured bend values are, nonetheless, consistent with the fit from the AGN with well defined PSD bend timescales. Similarly we also plot the blazar 3C 273 (M^cHardy et al, in preparation, and Sect. 7 here) and the radio galaxy 3C 120 ([74] and Marshall et al, in preparation), which were also not included in the fit.

by simple linear transformation from X-ray flux, S_X . From that same Fig.3. [17] it can be seen that, in 2002, when the source was in a steady hard state, $\nu_{high} \propto S_X^{0.45 \pm 0.05}$. In hard state, jet dominated, systems, $S_X \propto \dot{m}_E^2$ [41]. Thus for the 2002, hard state, $\nu_{high} \propto \dot{m}_E^{0.9 \pm 0.1}$, i.e. the same dependence of timescale on accretion rate in an individual object that was previously found for the sample of AGN and BHBs.

In a comprehensive study it has been shown [34], using radio luminosity as a tracer of accretion rate in hard state objects [32], that hard state black hole systems and neutron stars also follow the same dependence of characteristic timescale with M_{BH} and \dot{m}_E that was derived earlier [53], which thus seems to be characteristic of the majority of accreting objects.

3.4 RMS variability as a mass diagnostic

From observations which are too sparse or too short to allow a well defined PSD to be produced, it is possible to estimate the bend timescale if we assume a particular, fixed, power spectral shape. The variance in a light curve, σ^2 , equals the integral of the power spectrum over the frequency range sampled by the light curve. Thus if we assume a fixed PSD shape, i.e. typically a fixed normalisation, low frequency slope and high frequency slope, then we can deduce the bend frequency from the observed variance in the light curve [e.g. 61]. This technique has been used to demonstrate a strong relationship between T_B and black hole mass but the dependence of T_B

on \dot{m}_E has not been clear [61, 58, 57]. The reason that the dependence on \dot{m}_E has not been clear in these analyses is probably that the samples under consideration did not contain a great range of accretion rates, with few NLS1s involved, and also that the assumption of a universal, fixed, PSD shape is not absolutely correct. Small differences in normalisation (e.g. compare NGC 3227 and NGC 5506 [82]) or in PSD slopes (the low frequency slope in MCG-6-30-15 is -0.8 whereas in NGC 4051 it is -1.0 [52, 55]) can easily move the derived bend frequency by half a decade, or more, which is sufficient to blur any dependence on accretion rate. High frequency PSD slope is also a function of energy, being flatter at higher energies [e.g. 55], and thus great care must be taken to ensure uniform energy coverage. Also, in the translation from σ^2 to T_B , a hard-state PSD shape has generally been assumed whereas we now know that a soft state is generally more likely.

Nonetheless, σ^2 does still provide a useful diagnostic of variability and has been used to good effect in the study of the evolution of variability properties with cosmic epoch. In an analysis of a deep ROSAT observation it has been shown [1] that, for a particular luminosity, the variance of high redshift ($z > 0.5$) QSOs was greater than that of low redshift QSOs. A similar, though more detailed, analysis has been performed [63] using the extensive *XMM-Newton* observations of the Lockman hole which show that, for the same luminosity, black hole mass is lower, but accretion rate is higher, for the higher redshift QSOs, indicative of the growth of black holes with cosmic epoch.

3.5 High frequency scaling relationships

Measurements of rms variability are usually carried out on individual observations lasting for maybe a day or so. These observations thus mainly sample the high frequency part of the PSD. There have been related methods of quantifying variability which also use the high frequency part of the PSD.

In the late 1980s we used the amplitude of the normalised PSD (after removing the Poisson noise level) at a standard frequency of 10^{-4} Hz (the ‘normalised variability amplitude’, *NVA*, [49] and [27]). This frequency was chosen to be as high as possible whilst avoiding the region dominated by Poisson noise in typical EXOSAT observations. At that time very few AGN black hole masses were available and so *NVA* had to be plotted against luminosity as a proxy, and *NVA* was seen to decrease with increasing luminosity. Subsequently, broadly similar techniques were used [30, 17] to show that high frequency variability timescales scaled approximately with mass.

Recently the PSDs of a number of hard-state BHBs have been studied and it is found that the high frequency part of the PSD does not change greatly with source flux [26] although the lower frequency part does change. It is surmised that the relatively unchanged high frequency tail part of the PSD may represent some limit, such as the last stable orbit, for the black hole in question. Nonetheless a plot of the amplitude of the PSD tail extrapolated to 1Hz (C_M - very similar to the *NVA* discussed above) against mass reveals no correlation with mass within the BHB sample alone. However if a sample of AGN [57] are included, estimating C_M from the variance by model fitting assuming a hard state PSD, there is a correlation with mass. As many AGN are probably soft state systems, and as the range of accretion rates in that AGN sample is small, further work is required to determine whether

the high frequency part of the PSD gives a mass measurement, independent of any accretion rate variations.

Overall, measures of variability timescale based solely on the high frequency part of the PSD can provide a reasonable mass estimate for many AGN samples where there is not a great range in accretion rate. Future work may show that they give an accretion-rate independent measure of mass, but that is not yet confirmed. These methods have the advantage of being applicable to short observations. However measurement of the PSD bend timescale is more robust to changes of PSD slope and normalisation and provides a more sensitive diagnostic of mass and accretion rate.

4 Relationship between nuclear variability properties and larger scale AGN properties

One of the more important observable AGN parameters is the width of their permitted optical emission lines, V . This linewidth is often used as a means of classifying different types of AGN. It has been shown that the most variable X-ray emitting AGN (where variability has typically been quantified in terms of σ_{rms}), tend to have the narrowest optical emission lines [e.g. 78]. However there is a good deal of spread in the relationship between σ_{rms} and V , and no quantitative physical explanation of the relationship has yet been forthcoming.

In Fig 6 we show a plot of linewidth, V , against T_B [53]. Here we note a remarkably tight relationship. Parameterizing $\log T_B = D \log V + E$, we found that $D = 4.2^{+0.71}_{-0.56}$ [53]. Such a tight relationship should have a simple explanation and, indeed, such an explanation can be derived from simple scaling relationships.

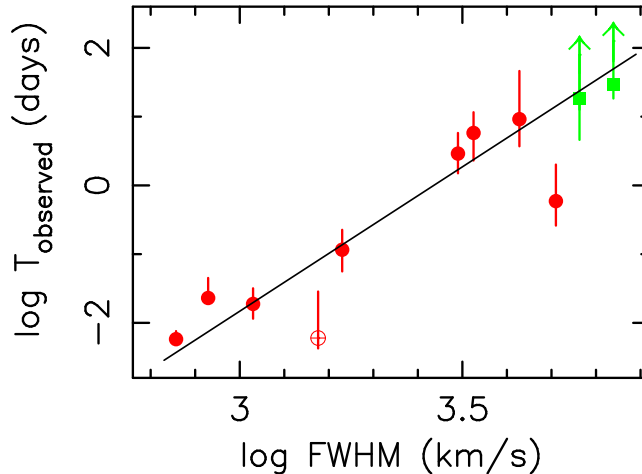


Fig. 6. Correlation of the observed PSD bend timescale vs. the FWHM of the H_β optical emission line.

We assume that the linewidth arises from the Doppler motions of neutral gas at the inner edge of the broad line region (BLR), and that the BLR is excited by radiation from the central black hole. If the gas is in virial motion then $V^2 \sim GM_{BH}/R_{BLR}$, where R_{BLR} is the radius of that inner edge. We assume that the ionising luminosity, $L \sim M_{BH} \dot{m}_E$. For the locally optimised condition for the production of emission lines by gas at the same optimum density and ionisation state we expect $R_{BLR} \propto L^{0.5}$ and measurements of the radius of the BLR confirm that expectation, finding that $R_{BLR} \propto L^{0.518 \pm 0.039}$ [9]. Putting these simple scaling relationships together we then expect that $V^4 \sim M_{BH}/\dot{m}_E$. As it has already been shown that $T_B \sim M_{BH}/\dot{m}_E$, then we naturally explain the observation that $T_B \sim V^4$ and, by self-consistency, we show that the basic assumptions that we have made above about the BLR are probably correct.

We therefore have a strong link between small scale nuclear accretion properties (X-ray variability) and larger scale properties of the AGN (linewidth). The relationship shown in Fig 6 is particularly useful as it is purely a plot of two observational quantities, and does not rely on any assumptions or derivations. Thus from a simple measurement of an optical linewidth, we can make at least a first order prediction of how the X-ray emission from a Seyfert galaxy should vary.

5 Origin of T_B

We have now measured, reasonably well, the way in which T_B varies with M_{BH} and \dot{m}_E in all types of accreting systems. But what is the physical origin of T_B ? On timescales shorter than T_B , the variability power drops rapidly and so it is natural to associate T_B with some cut-off, or edge, in the accreting system. One obvious possibility, therefore, is the inner edge of the optically thick accretion disc. However, unless we push the inner edge of the disc out to much larger radii ($\gtrsim 20R_G$) than are considered reasonable for soft state systems [12], the simple dynamical timescale, T_d , at the edge of the disc is much shorter than the observed PSD bend timescale. Other possible characteristic timescales are the thermal timescale, $T_{therm} = T_d/\alpha$, where α is the viscosity parameter, typically taken to be ~ 0.1 , and the viscous timescale, $T_{visc} = T_{therm}/(H/R)^2$, where H/R is the ratio of the scale height to radius of the disc [76].

For any fixed black hole mass, the viscous timescale, as well as the dynamical timescale, can be varied only by varying the inner disc radius (assuming that the viscosity parameter does not change). Measurements of the disc radius, usually by means of spectral fitting to the disc spectrum (e.g. [12]), show that the inner disc radius is large at low accretion rates, and decreases as the accretion rate rises. However once the accretion rate exceeds a few percent of the Eddington accretion rate (i.e. typically in soft states), the radius has typically decreased to a few gravitational radii and it is hard to measure further changes with increasing accretion rate. Although such measurements are prone to large uncertainties, nonetheless there does not yet seem to be evidence for the large changes of radius with accretion rate that would be required to explain the spread of timescales, for a given black hole mass, that are observed [e.g. 52].

The viscous timescale can, however, be changed, for the same radius, by altering the scale height of the disc. If we assume that, when in the soft state, the inner edge of the accretion disc reaches to the innermost stable orbit at, say $1.23R_G$ (the limit

for a maximally spinning Kerr black hole), and that the observed bend timescale is actually a viscous timescale at that radius, then we can derive the scale height of the disc (H/R). We then find that H/R varies between about 0.1 for $\dot{m}_E \sim 0.01$ to about unity at $\dot{m}_E \sim 1$, which is a sensible range, broadly in line with theoretical expectations. Thus T_B might well be associated with the viscous timescale at the inner edge of the accretion disc: that edge firstly moves in as the accretion rate rises in the hard state, and then, once the edge has reached the innermost stable orbit, further rises in accretion rate increase H/R .

6 Origin of the Variations

We have seen that AGN and BHBs have similar ‘states’ and display similar patterns of variability. We have found scaling relationships which enable us to link the timing properties of accreting objects of all masses. We are beginning to have some idea of the origin of the main characteristic timescale in AGN. But what is the underlying origin of the variability?

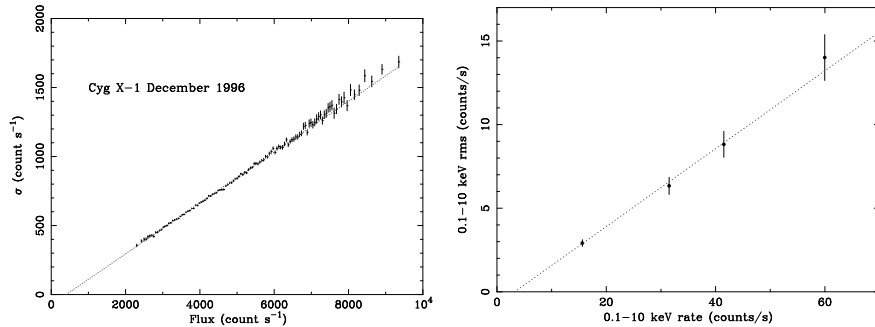


Fig. 7. Left panel: rms-flux relationship for Cyg X-1 [81]. Right panel: rms-flux relationship for the Seyfert galaxy NGC 4051 [55]

6.1 Shot-noise models

A model commonly-used to describe variability is the random shot noise model. In this model, light curves are made up of the superposition of pulses, or shots, randomly distributed in time. If all of the shots have the same decay timescale then we have white noise. However if we allow for a range of decay timescales then we can reproduce the bending powerlaw PSDs seen in BHBs and AGN [6, 37, 50]. Also, if more luminous sources simply contain more shots, then the fractional variability of more luminous sources will be less than that of less luminous sources. This behaviour is generally seen but from the fact that the normalised variability amplitude, NVA , decreases with increasing luminosity less slowly than would be expected for random, similarly sized, shots (i.e. we see $NVA \propto L^{-0.34}$ rather than the expected $NVA \propto L^{-0.5}$), it was concluded that if the variability does arise from the summed emission

from a number of separate regions, then there must be some correlation between those regions [27].

6.2 The rms-flux relationship

Although shot noise models can explain the shape of the power spectra, they cannot explain the way in which the rms variability of the light curves varies with flux. Following some discussions regarding the benefits of calculating PSDs in absolute or rms units, it was noted that the rms variability of the light curves is directly proportional to the flux [81]. This proportionality is now known as the rms-flux relationship. In Fig. 7 we show the rms-flux relationship for the BHB Cyg X-1 [81] and for the Seyfert galaxy NGC 4051 [55]. This linear relationship has now been found in all BHBs and AGN for which the observations were sufficient to define it. We incidentally note that the rms-flux relationship usually does not go through the origin but has a positive intercept on the flux axis at zero rms, indicative of a constant (e.g. thermal) component to the X-ray flux.

The important implication of the rms-flux relationship is that when the long timescale Fourier components of the light curve, which determine the overall average flux level, are large, the short timescales components, which determine the rms variability, are also large, and vice versa. Thus different timescales know about each other.

In simple additive shot noise models the shots are independent and so the rms will be constant and independent of flux. Simulations show that a random distribution of similar shots will not reproduce the extended low-flux periods seen in NGC 4051 [29, 80], i.e. the short timescale variability knowing that the average long timescale flux is very low. In simple shot noise models at least one large shot will always appear in the low flux periods. As the rms/flux relationship applies, at least to BHBs, on whichever timescale one measures the rms (e.g. 1s, 10s bins etc), then to make shot noise models produce the rms-flux relationship, we would have to introduce some mechanism which alters the shot amplitude on a large variety of timescales. What that mechanism would be is unknown and hence we are really no further forward in our understanding.

6.3 Propagating fluctuation models

An alternative, and simpler, explanation of the rms-flux relationship is provided by the propagating fluctuation model, initially proposed by Lyubarskii [38]. In this model fractional variations in mass accretion rate are produced on timescales longer than the local viscous timescale so that longer timescale variations are produced further out in the accretion disc. These variations then propagate inwards. If the low frequency variations then modulate the amplitude of higher frequency variations produced closer in (as in amplitude modulation in radio communications) then we produce a linear rms-flux relationship. Note that this relationship between frequencies is multiplicative, not additive. If each inner frequency is modulated then by the product of all lower frequency modulations produced further out, then the rms-flux relationship will apply no matter what frequency range one chooses to measure the rms over, or at which lower frequency one chooses to measure the flux.

There are a number of implications when the time series is produced by multiplying together a set of variations of different frequencies. First let us consider the distribution of fluxes. If a light curve is produced by the sum of many random sub-processes then, by the central limit theorem, the fluxes will be normally distributed, i.e. they will follow a Gaussian distribution. Summative processes are linear [e.g. 69], i.e. multiplying the input (e.g. the accretion rate) by some constant will multiply the output (e.g. the luminosity) by the same factor. However if a light curve is produced by the product of many random sub-processes, then the flux distribution will be lognormal (ie the distribution of the log of the fluxes will be Gaussian). The flux distributions of the well measured BHBs such as Cyg X-1 do indeed follow such a lognormal distribution. (A full discussion of these topics is presented elsewhere [84].)

If the observed light curve is actually the product of variations on a variety of timescales, then it is straightforward to show [84] that the observed light curve is the exponential of an underlying linear light curve. The observed light curve is therefore non-linear. As the non-linearity arises from the coupling between variations on different timescales, being ultimately driven by the lowest frequency variations (from the outer part of the disc, in the Lyubarskii model), then the larger the driving variations are, the greater will be the non-linearity. In Fig. 8 I show examples of light curves simulated using the exponential formulation, with increasing rms variability (from top to bottom) but with similar random number sequence used in their generation. It can clearly be seen how the light curves become more non-linear as the rms variability increases. The lower rms variability light curves are typical of many ordinary Seyfert galaxies whilst the higher rms, more non-linear, light curves are typical of the NLS1s.

A qualitative model which can explain many of the spectral timing observations of AGN and BHBs has been proposed [15, 35]. In this model the $1/f$ power spectrum of variations which is produced in the Lyubarskii model propagates inwards, perhaps in an optically thin corona over the surface of the disc, until it hits the X-ray emitting region, whose emission it modulates. A numerical version of this model has been developed [3] which can reproduce many observed aspects of X-ray spectral variability. The critical aspects of these models is that the source of the variations is not the same as the source of the X-rays.

Lags and Coherence

As well as providing an indication of X-ray state (Sect. 2), lags and coherence are potentially very powerful diagnostics of emission models and geometry. A standard interpretation of the lag of the soft band by the hard band is given by Comptonisation models. In these models the low energy seed photons from the accretion disc are Compton-scattered up to higher energies by a surrounding corona of very hot electrons. As more scatterings are required to reach the higher energies, the higher energy X-rays will be delayed relative to the lower energy photons.

However there are other observed aspects of X-ray variability which are not so easily explained by simple Comptonisation scenarios, e.g. the observation that the slope of the PSD above the bend is flatter for most AGN at higher energies (eg Fig. 9). If the variability is driven by variations in the seed photons, one would expect high frequency variability to be washed out by many scatterings and so would expect the PSD to be steeper above the bend at higher frequencies. We might retain the

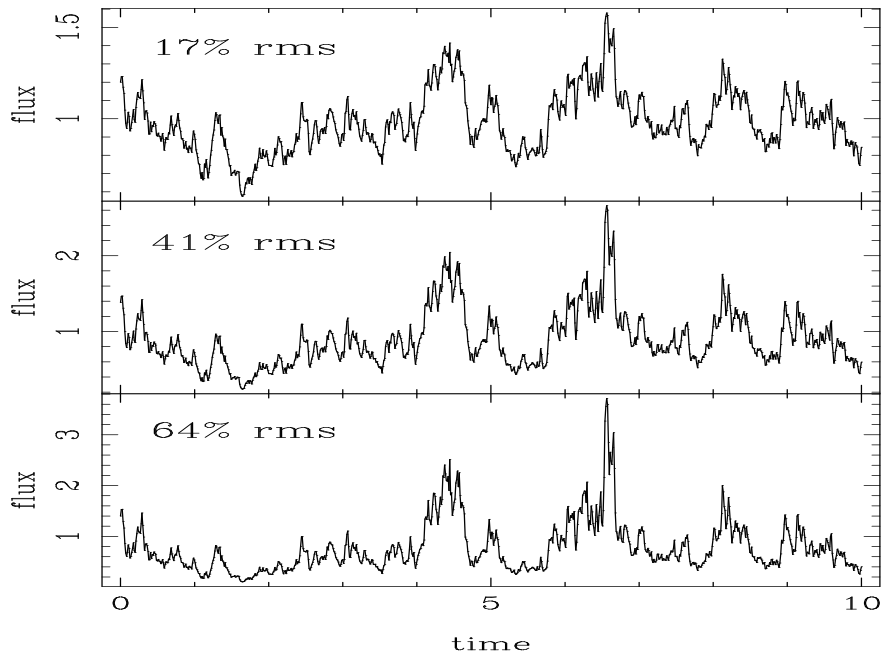


Fig. 8. Simulated exponential light curves [84] showing increasing non-linearity as the rms variability increases.

Comptonisation model if the high frequency variability is driven by variations in the corona rather than in variations in the seed photon flux. However the temperature and optical depth of the corona would have to be carefully tuned so that seed photons are raised to high energies by very few scatterings and are then immediately able to leave the corona.

A perhaps more natural explanation of the lags, the coherence and the energy-dependent PSD shapes can be provided by the propagating fluctuations scenario if we introduce an X-ray emitting region with a hardness gradient, such that higher energy X-rays are emitted, preferentially, closer in towards the black hole [35]. The geometry of the emission region is not critically defined but might extend over the inner region of the accretion disc. The overall emissivity at all energies would still rise with decreasing radius, perhaps $\propto r^{-3}$, in accordance with the expectation for the release of gravitational potential energy, but the proportion of higher energy photons released would increase with decreasing radius. If viewed from far out in the accretion disc, there would thus be an emission-weighted centroid for each energy, and this centroid would move to larger radius as the energy decreases. The observed lag between the hard and soft bands would therefore simply represent the time taken for the incoming perturbations to travel between the centroids of the particular soft and hard energy bands under consideration.

This scenario can also explain why the lags vary with the Fourier frequency of the perturbations. The lowest frequency perturbations will originate far beyond any X-ray emission region and so will produce the largest possible lag. The lag

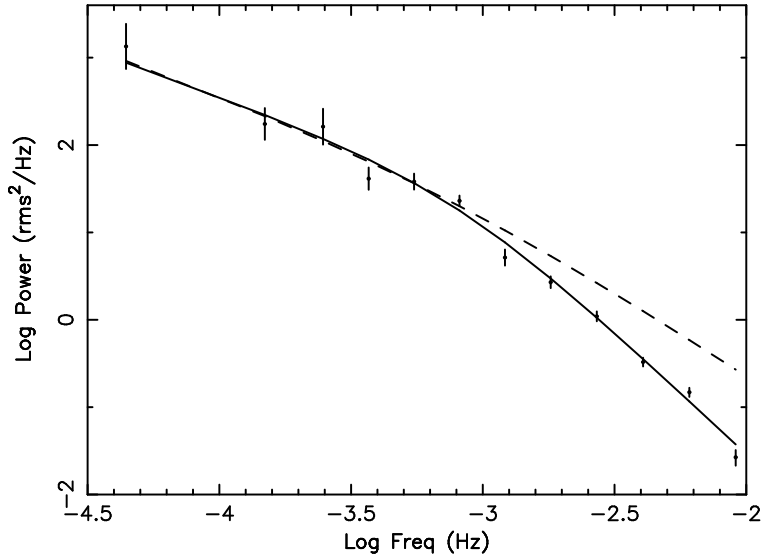


Fig. 9. PSDs of NGC 4051 from *XMM-Newton* observations. The data are from the 0.2-2 keV band and the solid line is the best fit to these data. The dashed line is the fit to the 2-10 keV PSD. Note that this PSD is flatter than that of the 0.2-2 keV PSD at higher frequencies. (The normalisation of the 2-10 keV PSD has been slightly increased to make it the same as that of the 0.2-2 keV PSD at low frequencies.)

will remain the same as we move to higher frequencies until we reach frequencies which are produced within the X-ray emission region. Once we move inside the X-ray emission region then the centroid of the remaining emission from smaller radii (i.e. the emission that can still be modulated by the perturbations from further out) will move to smaller radii. As the radial profile of the X-ray emission will be more extended at lower energies, the centroid of the lower energy emission will move inwards more than the centroid of the higher energy emission. Therefore the lag will decrease as we move to higher frequencies (e.g. NGC 4051, [55]).

In Akn 564 we note (Fig 1) that, at the very highest frequencies, the lags are slightly negative (-11 ± 4.3 s [51]), i.e. the hard band leads. In the model discussed here the very high frequencies are produced in the region where the X-ray source is very hard. The main source of soft photons in this region may therefore not be the intrinsic source spectrum but may come from reprocessing of the intrinsic very hard spectrum by the accretion disc. The lag may then represent approximately twice the light travel time between the hard X-ray corona and reprocessing accretion disc.

By altering the emissivity profile of the disc it is possible to produce lags which vary as a function of frequency either smoothly (as in NGC 4051 or Mkn 335, e.g. Fig. 10 [2]) or in a stepwise manner (e.g. Akn 564, [51]). The propagating fluctuation model can simultaneously explain the energy-dependent shape of the PSDs, thereby providing a simple and self-consistent explanation of many spectral-timing properties of accreting systems.

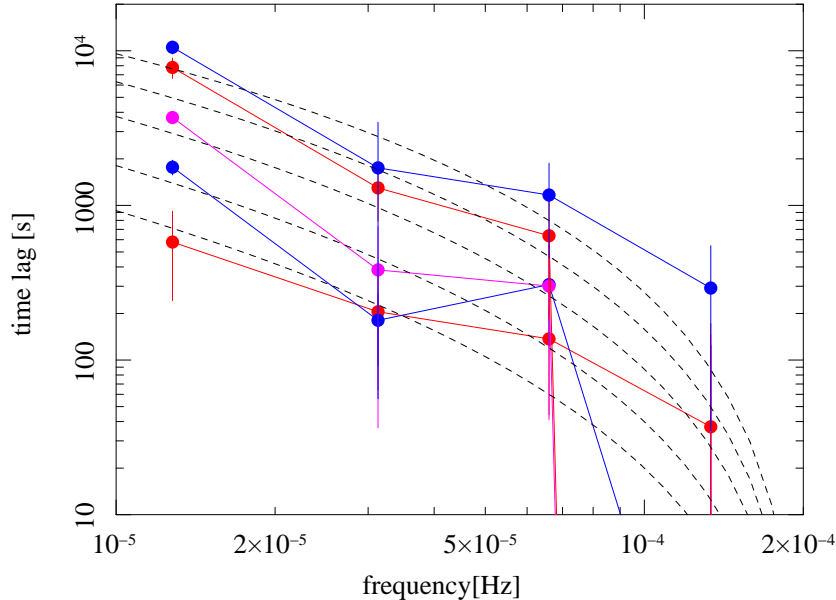


Fig. 10. The data points show the time lag, as a function of Fourier frequency, between the 0.2-0.4 keV band and the 0.4-0.6, 0.6-1, 1-2, 2-5 and 5-10 keV bands for Mkn 335. The lags increase as we move to larger energy separations and in all cases the hard band lags behind the soft band. The faint dashed lines represent model fits to these data based upon the propagating fluctuation scenario with a disc emissivity profile (at least in the 0.2-0.4 keV band) $\propto r^{-3}$ and the inner edge of the optically thick disc being truncated at $6R_g$ [2].

We note that the truncation of the optically thick disc leads to a rapid drop in the lags at a frequency close to the bend in the PSD. Although we do not yet have accurate lag measurements for many AGN, the indications are that the lag drops follow the same mass (and possibly accretion rate) scaling that is found for the PSD bend timescales.

7 Variability of Blazars

The radio through optical emission in blazars like 3C 273 and 3C 279, ie AGN with apparent superluminal radio components, is synchrotron emission from a relativistic jet oriented at a small angle to the line of sight. In 3C 273 the tight correlation between the synchrotron component (e.g. IR) and X-rays, with the X-rays lagging the synchrotron by \sim day [e.g. 48], indicates that the X-ray emission mechanism is almost certainly synchrotron self-Compton (SSC) emission from the jet [e.g. 72, 48]. A similar mechanism probably applies in all other blazars. Thus the X-ray emission region (in a relativistic jet) and emission process are different to those of Seyfert galaxies where the X-ray emission is not relativistically beamed and the emission

process is probably a thermal Compton emission process. It is therefore not at all clear that we should expect similar X-ray variability characteristics.

3C 273 is one of the brightest AGN in the sky and, as such, has been observed by all major observatories since the 1970s. We have collected these data, including extensive observations with *RXTE*, and the long term light curve is shown in Fig 11a. Using PSRESP, in our normal manner, I have made the PSD which is shown, unfolded from the distortions introduced by the sampling pattern, in Fig 11b. It can be seen that this PSD is exactly like that of a soft state Seyfert galaxy PSD. The bend timescale is 10 days. I have placed this observed timescale together with the predicted bend timescale onto Fig. 5. For comparison with most of the other non-beamed AGN on that figure we use the black hole mass derived from reverberation measurements by the same observers [66]. It can be seen that 3C 273 fits the scaling relationship between M_{BH} , \dot{m}_E and T_B as well as all the Seyfert galaxies.

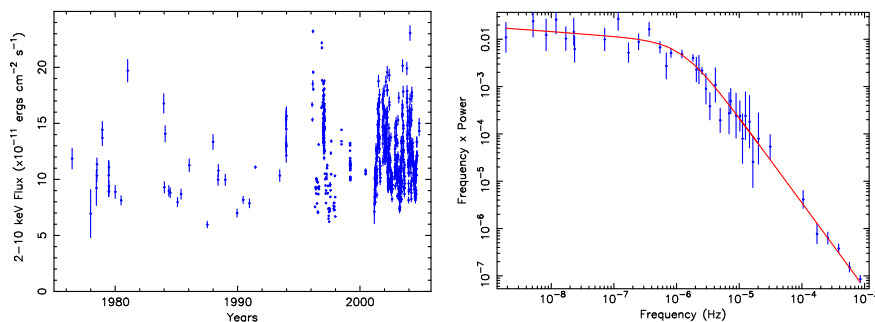


Fig. 11. (a) Left panel: Long term 2-10 keV X-ray lightcurve of 3C 273. The intensive monitoring after 1996 is from *RXTE*; the earlier data are from the Ariel V SSI, Exosat and Ginga. (b) Right panel: Unfolded PSD of the blazar 3C 273, showing an excellent fit to the same bending powerlaw model that fits the Seyfert galaxies (M^cHardy et al, in preparation)

We note that there is no necessity to alter the observed bend timescale by any relativistic time dilation factor to make the observed bend timescale fit with the relationship derived for Seyfert galaxies and BHBs. For a clock moving with the jet of 3C 273, that factor would be about 10. The implication, therefore, is that the source of the variations - note, not the source of the X-rays - lies outside the jet and is simply modulating the emission from the jet. Coupled with the fact that the PSD of 3C 273 looks exactly like that of soft state Seyfert galaxies and BHBs, this implication is then entirely consistent with Seyfert galaxies, BHBs and blazars all suffering the same sort of variations, e.g. variations propagating inwards through the disc. The jet then would be seen as an extension of the corona which dominates the emission in Seyfert galaxies.

rms-flux relationship for 3C 279

3C 279 is an even more relativistically beamed blazar than 3C 273 [e.g. 14]. For both of these objects we have calculated the rms-flux relationship from the *RXTE*

monitoring observations. Both objects show a strong linear relationship (e.g. Fig 12). This relationship provides strong confirmation that the underlying process driving the variability in blazars has the same multiplicative relationship between different frequencies that is seen in BHBs and Seyfert galaxies. Coupled with our observation that the PSD shape of 3C 273 is identical to that of Seyfert galaxies, the simplest conclusion is that the process driving the variability in all systems is the same, i.e. fluctuations propagating inwards through the disc.

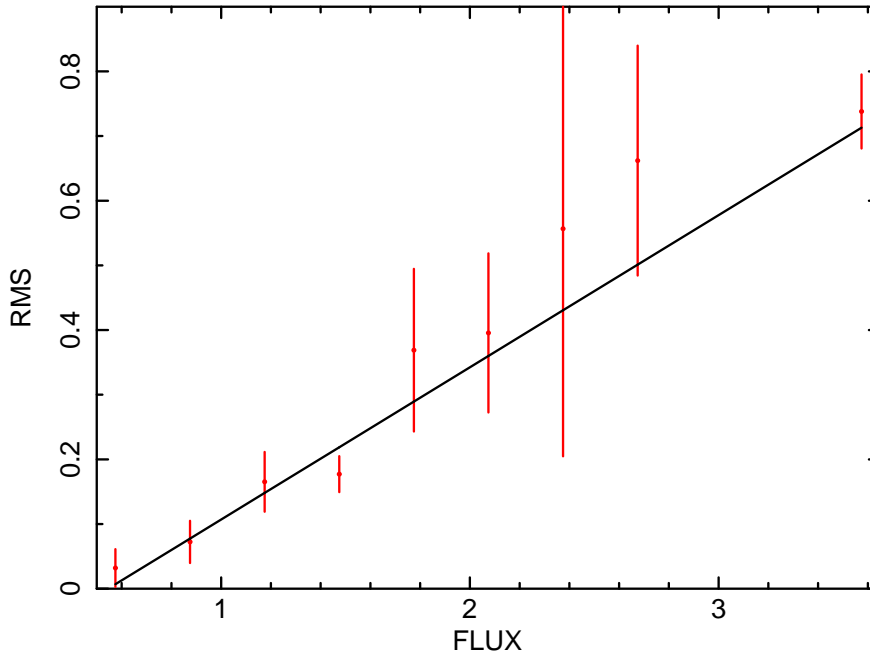


Fig. 12. RMS-Flux relationship for 3C 279 with flux and rms both being measured in the 2-10 keV band in units of 10^{-11} ergs cm^{-2} s^{-1} .

8 X-ray/Optical Variability

For many years the origin of the optical variability of AGN has been, at best, a mystery and, at worst, a complete muddle. It has often been suggested that optical variability arises from reprocessing of X-ray variations but most early X-ray/optical studies found either weak [67] or non-existent [19] X-ray/optical correlations. In the case of NGC 3516 a strong correlation appeared to exist in the first set of observations, with the optical leading the X-rays by 100d [39], but this correlation was not confirmed by subsequent observations [40]. However during a 100ksec *XMM-Newton* observation of NGC 4051, the UV (2900Å) emission was observed to lag behind the X-rays by $\sim 0.2\text{d}$ [43]. The optical variability amplitude was much less than that of the X-rays, consistent with reprocessing.

Our understanding of X-ray/optical variability has, however, improved considerably recently due largely to the long timescale *RXTE* X-ray monitoring programmes of ourselves and others, coupled with extensive optical monitoring programmes from groups such as AGNwatch and from robotic optical telescopes. In the case of NGC 5548 a strong X-ray/optical correlation has also been found [79] but here the optical band varies at least as much as the X-rays, which is energetically difficult to achieve with reprocessing. NGC 5548 has a more massive black hole ($10^8 M_\odot$) than NGC 4051 ($10^6 M_\odot$) or NGC 3516 ($4.3 \times 10^7 M_\odot$), prompting thoughts that the correlation might be mass dependent. In higher mass (or lower accretion rate) black hole systems the disc temperature is lower (for a given radius, in terms of gravitational radii). Thus the optical emitting region will be closer to, and will subtend a greater solid angle at, the central X-ray emitting source. This geometry would increase the efficiency of reprocessing but would also mean that both optical and X-ray emitting regions would be subject to more similar variations than if they were widely separated. Recent X-ray/optical monitoring of MR 2251-178 [4] another high mass AGN ($10^8 M_\odot$), finds a similar pattern to that of NGC 5548. However in the case of Mkn 79 [11] ($10^8 M_\odot$) we see correlated X-ray and optical variations on short timescales (tens of days, Fig. 13) but large amplitude changes in the optical band on \sim years timescales which are not seen in the X-ray band.

If we remove the long term trend in the optical light curve of Mkn 79, we find an extremely strong ($> 99.5\%$ significance) correlation between the X-ray and optical variations with a lag very close to zero days ($\pm \sim 2$ d). Similar behaviour is seen in other AGN of medium or low black hole mass (Breedt et al, in preparation). This correlation provides strong support for the model in which the short timescale optical variability in AGN is dominated by reprocessing of X-ray photons. This result is consistent with the observations of wavelength dependent lags between different optical bands in AGN [13, 71] which are also best explained by reprocessing.

However the slower optical variations in both MR 2251-178 [4] and Mkn 79 [11] cannot be explained by reprocessing from an X-ray emission region on an accretion disc both of constant geometry. As reprocessing from the accretion disc occurs on the light travel time which is, at most, a few days, it is impossible to remove all of the fast variations seen in the X-ray band. It might be possible to produce very smooth reprocessed light curves if the reprocessor is much larger than the accretion disc, e.g. if it is in the broad line region or torus. Another possibility is that the slow optical variations can be explained either by varying the accretion rate in the disc, or by varying the geometry of the X-ray source or accretion disc. The radius within which half of the thermal optical emission from the accretion disc in Mkn 79 is produced is $70R_G$. The viscous timescale at this radius is about 4.7 years. Thus variations in accretion rate, propagating inwards, would be expected to vary the intrinsic thermal emission from the disc on that sort of timescale, which is consistent with the optical long term trends seen in Fig 13. Alternatively, if we approximate the X-ray emitting corona as a point source at its centroid, above the accretion disc, we can change the strength of the reprocessed optical signal by altering the height of that point source. We can also alter the strength of the reprocessed signal by changing the inner radius of the accretion disc. Further work is underway to determine which of these possibilities is the most likely.

We note that a variable height lamppost model has been invoked to explain continuum variability coupled with much lower variability of the iron line in MCG-6-30-15 [46]. When the source is close to the disc, a greater fraction of the continuum

is gravitationally bent back to the disc or into the black hole, thereby reducing the flux as seen by a distant observer but not altering the reprocessed iron line flux greatly. Although a reasonable explanation of spectral variability, this model cannot explain the rms-flux relationship where the observed variability is least at the lowest continuum fluxes.

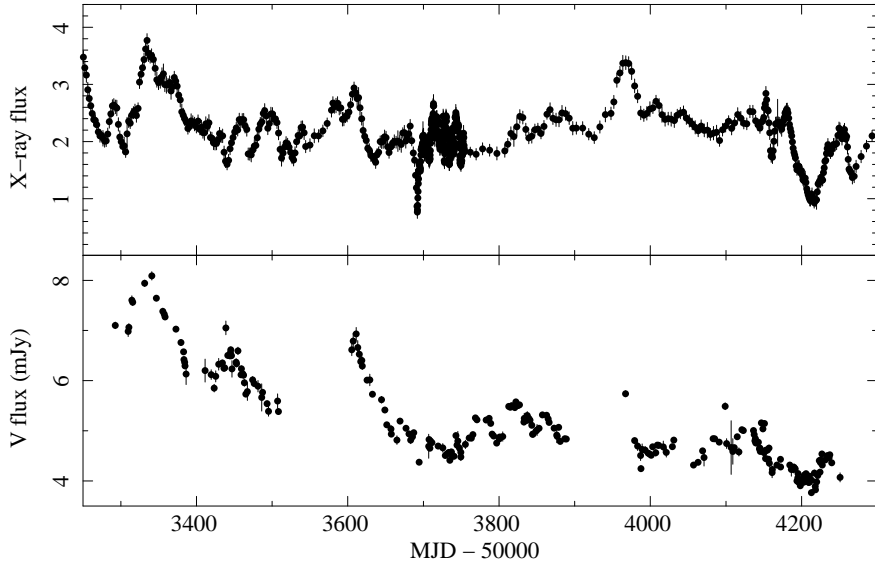


Fig. 13. Optical and X-ray variations in Mkn 79 [11]. Note how the variations are correlated on short timescales (weeks/month), probably showing that the optical variations arise from reprocessing of the optical emission. However the optical emission varies independently on longer timescales, possibly indicating changes in the intrinsic emission from the disc due to accretion rate changes or possibly indicating changes in the geometry of the X-ray source.

9 Conclusions

Our understanding of AGN variability has improved enormously in the last 20 years and the analogy with BHBs is now very strong. Almost all of the bright AGN with well measured PSDs have PSDs similar to those of Cyg X-1 in the soft state. These AGN typically have accretion rates similar to those of soft state BHBs. Akn 564, which has a very high accretion rate, perhaps even exceeding the Eddington limit, has a PSD similar to that of BHBs in the very high state where accretion rates are similarly high. Ton S180, another very high accretion rate AGN, has a less well measured PSD which is also similar to that of a VHS BHB. As yet we have no firm evidence, from PSD shapes, for a hard-state AGN, but this result is probably just due to two selection effects. Hard-state BHBs have low accretion rates ($<2\% \dot{m}_E$)

and so have low X-ray luminosities. Thus, unless they are very nearby, hard state AGN will be too faint to detect with dedicated monitoring satellites such as RXTE. Secondly, in order to confirm a hard PSD state, one must detect the second bend, at low frequency, to a slope of zero and, as bend frequencies scale inversely with accretion rate, typical bend timescales will be far too long to be measured within a human lifetime.

Measurement of the lags between different energy bands as a function of Fourier timescale provides another strong state diagnostic and in the very high accretion rate AGN Akn 564 we see a lag spectrum very similar to that seen in very high accretion rate BHBs. In particular, we see a rapid change in lag at the frequency at which the PSD changes from being dominated by one Lorentzian shaped component to another, again, just as in BHBs.

Characteristic timescales in accreting systems have now been shown to vary almost exactly linearly with compact object mass and inversely with accretion rate (in Eddington units). This scaling relationship applies over a huge range of over 10 decades in timescale. The physical origin of the high frequency bend in the PSD is not yet entirely clear but is very likely related to a timescale, probably viscous, at the inner radius of the optically thick part of the accretion disc. This radius probably moves inwards with rises in accretion rate during the hard state but, in the soft state, it may hit the ISCO where an increase in disc scale height with increasing accretion rate could explain the decreasing characteristic timescales.

The fact that the relationship $T_B \propto M_{BH}^{1.12} / \dot{m}_E^{0.98}$ is a good fit within the measurement errors without having to invoke an additional unknown source of error indicates that no other parameters besides M_{BH} and \dot{m}_E have a major effect on determining T_B . If T_B is associated with the inner edge of the accretion disc then an obvious additional parameter would be spin, which alters the radius of the last stable orbit and hence of all associated timescales. The implication of the good fit is therefore that the spin of all black holes whose accretion rate is high enough for them to be powerful X-ray sources is broadly similar.

The discovery of the rms-flux relationship in both AGN and BHBs shows that the process underlying the variability is multiplicative, rather than additive. Thus the amplitude of the shorter timescale variations are modulated by the amplitude of the longer timescale variations, leading to occasions (e.g. in NGC 4051) where the X-ray flux almost completely turns off. Standard shot noise models, with independent shots, are thus ruled out. The rms-flux relationship predicts a lognormal flux distribution, which is seen in BHBs where the count rate is high enough for reliable measurement. The link between variations on different timescales implies that the light curves will be non-linear, with the greatest non-linearity in the sources with the highest rms variability, exactly as is seen, e.g. in the narrow line Seyfert 1 galaxies.

The physical models which best explain the overall patterns of X-ray variability, i.e. the PSD shape, the lag spectra and the coherence between different energy bands, are those in which the production of the variations is separated from the production of the X-rays. Thus accretion rate variations in the accretion disc [e.g. 38] may propagate inwards and modulate an X-ray emission region with an energy-stratified emission profile [e.g. 35, 15].

The origin of optical variability in Seyferts, and its relationship to the X-ray variability, is also partly explained by propagating fluctuations. Although short-timescale (few days/weeks) optical variability is well explained by X-ray reprocessing, longer timescale optical variations, which have no parallel in the X-ray band,

may result from perturbations propagating inwards through the accretion disc which may take many years to travel from the optical to X-ray emission region.

There is some evidence that the same general pattern of variability that is seen in the non-relativistically beamed AGN and BHBs is also seen in blazars. The X-ray emission mechanism in blazars (eg synchrotron self-Compton emission) is almost certainly different to that in Seyfert galaxies (probably thermal Comptonisation) but blazars also demonstrate the rms-flux relationship and, in at least one well-observed case (3C 273) the PSD shape is identical to that of soft-state Seyfert galaxies. Moreover the characteristic PSD timescale in 3C 273 is entirely consistent with that expected, based on its black hole mass and accretion rate, from Seyfert galaxies, without any requirement for modification to take account of the relativistic motion of the emitting region. The conclusion, therefore, is that the source of the variations lies outside the jet, whose emission it modulates, and that that source is probably the same as in BHBs and Seyfert galaxies.

A major task for future observatories is to extend the variability studies of Seyfert galaxies to galaxies of very low accretion rate (ie $< 1\% \dot{m}_E$). The aims are to determine whether such AGN are hard state systems, whether the transition accretion rate in AGN is the same as, or different to, that in BHBs and whether such AGN behave in exactly the same way as scaled-up hard state BHBs. However such AGN are likely to be faint and the required monitoring timescales will be long. Thus I encourage the building of a sensitive (sub-mCrab on \sim day timescales) all-sky X-ray monitor, with few arcmin resolution to avoid confusion problems and with a lifetime of ~ 10 years rather than the ~ 2 years typical of many missions.

References

- [1] O. Almaini, A. Lawrence, T. Shanks et al.: MNRAS, **315**, 325 (2000)
- [2] P. Arévalo, I. M. McHardy, D. P. Summons: MNRAS, **388**, 211 (2008)
- [3] P. Arévalo, P. Uttley: MNRAS, **367**, 801 (2006)
- [4] P. Arévalo, P. Uttley, S. Kaspi et al.: MNRAS, **389**, 1479 (2008)
- [5] M. Axelsson, L. Borgonovo, S. Larsson: A&A, **438**, 999 (2005)
- [6] T. Belloni, G. Hasinger: A&A, **227**, L33 (1990)
- [7] T. Belloni, J. Homan, P. Casella et al.: A&A, **440**, 207 (2005)
- [8] T. Belloni, This Volume (2009).
- [9] M. C. Bentz, B. M. Peterson, R. W. Pogge et al.: ApJ, **644**, 133 (2006)
- [10] R. D. Blandford, A. König: ApJ, **232**, 34 (1979)
- [11] E. Breedt, P. Arévalo, I. M. McHardy et al.: MNRAS, **394**, 427 (2008)
- [12] C. Cabanac, R.P. Fender, R.J.H. Dunn et al.: MNRAS, in press (arXiv:0904.0701) (2009)
- [13] E. M. Cackett, K. Horne: MNRAS, **365**, 1180 (2006)
- [14] R. Chatterjee, S. G. Jorstad, A. P. Marscher et al.: ApJ, **689**, 79 (2008)
- [15] E. Churazov, M. Gilfanov, M. Revnivtsev: MNRAS, **321**, 759 (2001)
- [16] W. Cui, W. A. Heindl, R. E. Rothschild et al.: ApJ, **474**, L57 (1997)
- [17] C. Done, M. Gierliński: MNRAS, **364**, 208 (2005)
- [18] C. Done, G. M. Madejski, R. F. Mushotzky et al.: ApJ, **400**, 138 (1992)
- [19] C. Done, M. J. Ward, A. C. Fabian et al.: MNRAS, **243**, 713 (1990)
- [20] R. Edelson, K. Nandra: ApJ, **514**, 682 (1999)

- [21] A. A. Esin, R. Narayan, W. Cui et al.: *ApJ*, **505**, 854 (1998)
- [22] A. C. Fabian: *ApS&S*, **300**, 97 (2005)
- [23] H. Falcke, E. Körding, S. Markoff: *A&A*, **414**, 895 (2004)
- [24] R.P. Fender: This Volume (2009)
- [25] M. Gierliński, M. Middleton, M. Ward et al.: *Nature*, **455**, 369 (2008)
- [26] M. Gierliński, M. Nikolajuk, B. Czerny: *MNRAS*, **383**, 741 (2008)
- [27] A. R. Green, I. M. McHardy, H. J. Lehto: *MNRAS*, **265**, 664 (1993)
- [28] Q. Gu, J. Melnick, R. C. Fernandes et al.: *MNRAS*, **366**, 480 (2006)
- [29] M. Guainazzi, F. Nicastro, F. Fiore et al.: *MNRAS*, **301**, L1 (1998)
- [30] K. Hayashida, S. Miyamoto, S. Kitamoto et al.: *ApJ*, **500**, 642 (1998)
- [31] A. Herrero, R. P. Kudritzki, R. Gabler et al.: *A&A* **297**, 556 (1995)
- [32] E. G. Körding, R. P. Fender, S. Migliari: *MNRAS*, **369**, 1451 (2006)
- [33] E. G. Körding, Jester, S., R. P. Fender: *MNRAS*, **372**, 1366 (2006)
- [34] E. G. Körding, S. Migliari, R. Fender et al.: *MNRAS*, **380**, 301 (2007)
- [35] O. Kotov, E. Churazov, M. Gilfanov: *MNRAS*, **327**, 799 (2001)
- [36] A. Lawrence, M. G. Watson, K. A. Pounds et al.: *Nature*, **325**, 694 (1987)
- [37] H. J. Lehto: In: *Two Topics in X-Ray Astronomy*, Vol. 1, ed by J. Hunt and B. Battrick, volume 296 of *ESA Special Publication*, 499–503, (1989)
- [38] Y. E. Lyubarskii: *MNRAS*, **292**, 679 (1997)
- [39] D. Maoz, R. Edelson, K. Nandra: *AJ*, **119**, 119 (2000)
- [40] D. Maoz, A. Markowitz, R. Edelson et al.: *AJ*, **124**, 1988 (2002)
- [41] S. Markoff, H. Falcke, R. Fender: *A&A*, **372**, L25 (2001)
- [42] A. Markowitz, R. Edelson, S. Vaughan et al.: *ApJ*, **593**, 96 (2003)
- [43] K. O. Mason, I. M. McHardy, M. J. Page et al.: *ApJ*, **580**, L117 (2002)
- [44] A. Merloni, S. Heinz, T. di Matteo: *MNRAS*, **345**, 1057 (2003)
- [45] S. Migliari, R. P. Fender, M. van der Klis: *MNRAS*, **363**, 112 (2005)
- [46] G. Miniutti, A.C. Fabian, R. Goyder et al.: *MNRAS*, **344**, L22 (2003)
- [47] I. McHardy, B. Czerny: *Nature*, textbf325, 696 (1987)
- [48] I. McHardy, A. Lawson, A. Newsam et al.: *MNRAS*, **375**, 1521 (2007)
- [49] I. M. McHardy: *Mem S. A. It.*, **59**, 239 (1988)
- [50] I. M. McHardy: In: *Two Topics in X-Ray Astronomy*, Vol. 1, ed by J. Hunt and B. Battrick, volume 296 of *ESA Special Publication*, 1111–1124, (1989)
- [51] I. M. McHardy, P. Arévalo, P. Uttley et al.: *MNRAS*, **382**, 985 (2007)
- [52] I. M. McHardy, K. F. Gunn, P. Uttley et al.: *MNRAS*, **359**, 1469 (2005)
- [53] I. M. McHardy, E. Koerding, C. Knigge et al.: *Nature*, **444**, 730 (2006)
- [54] I. M. McHardy, I. E. Papadakis, P. Uttley: In *The Active X-ray Sky: Results from BeppoSAX and RXTE*, p. 509–514 (1998)
- [55] I. M. McHardy, I. E. Papadakis, P. Uttley et al.: *MNRAS*, **348**, 783 (2004)
- [56] N. M. Nagar, E. Oliva, A. Marconi et al.: *A&A*, **391**, L21 (2002)
- [57] M. Nikolajuk, B. Czerny, J. Ziółkowski et al.: *MNRAS*, **370**, 1534 (2006)
- [58] M. Nikolajuk, I. E. Papadakis, B. Czerny: *MNRAS*, **350**, L26 (2004)
- [59] M. A. Nowak: *MNRAS*, **318**, 361 (2000)
- [60] M. A. Nowak, B. A. Vaughan, J. Wilms et al.: *ApJ*, **510**, 874 (1999)
- [61] I. E. Papadakis: *MNRAS*, **348**, 207 (2004)
- [62] I. E. Papadakis, W. Brinkmann, H. Negoro et al.: *A&A*, **382**, L1 (2002)
- [63] I. E. Papadakis, E. Chatzopoulos, D. Athanasiadis et al.: *A&A*, **487**, 475 (2008)
- [64] I. E. Papadakis, I. M. McHardy: *MNRAS*, **273**, 923 (1995)
- [65] I. E. Papadakis, K. Nandra, D. Kazanas: *ApJ*, **554**, L133 (2001)
- [66] B. M. Peterson, L. Ferrarese, K. M. Gilbert, et al.: *ApJ*, **613**, 682 (2004)

- [67] B. M. Peterson, I. M. McHardy, B. J. Wilkes et al.: *ApJ*, **542**, 161 (2000)
- [68] K. Pounds, R. Edelson, A. Markowitz et al.: *ApJ*, **550**, L15 (2001)
- [69] M. B. Priestley: *Spectral Analysis and Time Series*, Academic Press, London (1982)
- [70] R. A. Remillard, J. E. McClintock: *ARA&A*, **44**, 49 (2006)
- [71] S. G. Sergeev, V. T. Doroshenko, Y. V. Golubinskiy et al.: *ApJ*, **622**, 129 (2005)
- [72] A. Sokolov, A. P. Marscher, I. M. McHardy: *ApJ*, **613**, 725 (2004)
- [73] D. P. Summons, P. Arevalo, I. M. McHardy et al.: *MNRAS*, **378**, 649 (2007)
- [74] D. P. Summons: PhD Thesis, University of Southampton (2007)
- [75] J. Timmer, M. Koenig: *A&A*, **300**, 707 (1995)
- [76] A. Treves, L. Maraschi, M. Abramowicz: *PASP*, **100**, 427 (1988)
- [77] S. P. Trudolyubov: *ApJ*, **558**, 276 (2001)
- [78] T. J. Turner, I. M. George, K. Nandra et al.: *ApJ*, **524**, 667 (1999)
- [79] P. Uttley, R. Edelson, I. M. McHardy et al.: *ApJ*, **584**, L53 (2003)
- [80] P. Uttley, I. M. McHardy, I. E. Papadakis et al.: *MNRAS*, **307**, L6 (1999)
- [81] P. Uttley, I. M. McHardy: *MNRAS*, **323**, L26 (2001)
- [82] P. Uttley, I. M. McHardy: *MNRAS*, **363**, 586 (2005)
- [83] P. Uttley, I. M. McHardy, I. E. Papadakis: *MNRAS*, **332**, 231 (2002)
- [84] P. Uttley, I. M. McHardy, S. Vaughan: *MNRAS*, **359**, 345 (2005)
- [85] B. A. Vaughan, M. A. Nowak: *ApJ*, **474**, L43 (1997)
- [86] N. E. White, A. C. Fabian, R. F. Mushotzky: *A&A*, **133**, L9 (1984)
- [87] J. Wilms, M. A. Nowak, K. Pottschmidt et al.: *A&A*, **447**, 245 (2006)
- [88] J. Ziółkowski: *MNRAS*, **358**, 851 (2005)